Second Year Activity Report

Giovanni Scala

Dottorato di Ricerca in Fisica, XXXIII ciclo

Dipartimento Interateneo di Fisica "M. Merilin"

Research activity

My second year of activity as phD student has been focused on the study of classical and quantum correlations, providing theoretical predictions for experiments, but also new generalizations in the framework of quantum entanglement. In the former activity, I follow the path started in my first year studying intensity correlations of light. The interest in this topic started in the mid fifties, when Hanbury-Brown and Twiss (HBT) proposed to measure the angular dimension of stars by retrieving second-order interference in the absence of first-order coherence. The debate concerning the interpretation, and even the correctness, of HBT's predictions was quite intense, due to the counterintuitive aspects related with the second-order interference arising from intensity correlation measurements. In fact, HBT intensity interferometry imposed a deep change in the concept of coherence, and triggered the development of quantum optics.
My activity involves also the search for general results on light-matter interactions for two-dimensional systems supporting plasmons. These plasmons effectively make the fine-structure constant larger and bridge the size gap between atom and light. This theory reveals that conventionally suppressed light-matter interactions such as extremely high-order multipolar transitions, two-plasmon spontaneous emission, and singlet-triplet phosphorescence processes can occur on very short time scales comparable to those of conventionally fast transitions. The idea is to take advantage of the full electronic spectrum of an emitter, and a potential testing ground for quantum electrodynamics (QED) in the media. While in the first line of research I studied the correlations in space, the mid-term objective of the latter is to analyze the correlations ofemitted light in the time-frequency domain. Moreover I am studying the quantumness, as non classical correlations from the abstract convex quantum state geometry.

Spatial correlations of the light for imaging and sensing

Correlation Plenoptic Imaging (CPI) is a novel imaging technique, that exploits the correlations between the intensity fluctuations of light to perform the typical

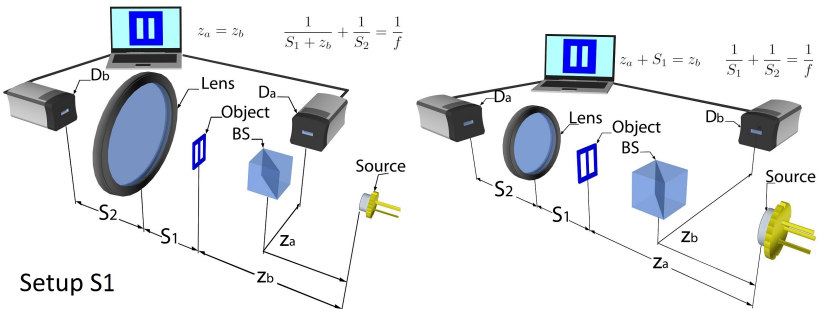

(a) (b)

Figure 1: Schematic representation of two setups that enable to perform plenoptic imaging by measuring correlations of intensity fluctuations $\Delta i(\boldsymbol{\rho}_a)\Delta i(\boldsymbol{\rho}_b)$ between points on two spatially resolving detectors D_a and D_b.

tasks of plenoptic imaging, namely refocusing out-of-focus parts of the scene, extending the depth of field, and performing 3D reconstruction. In this framework, I have characterized the noise properties, in particular the signal-to-noise ratio, of two setups aimed at performing plenoptic imaging with intensity correlations measurements. Both setups are illuminated by chaotic light, split in two paths by a beam splitter, and feature a transmissive object and a lens of focal length f. In setup S1 (upper panel), the chaotic source is focused by the lens on the detector D_b, while the "ghost" image of the object emerges in correspondence of D_a from the average $\Gamma(\boldsymbol{\rho}_a, \boldsymbol{\rho}_b) = \langle \Delta i(\boldsymbol{\rho}_a)\Delta i(\boldsymbol{\rho}_b)\rangle$. Setup S2 (lower panel) is based on a different working principle: the image of the object is formed by the lens on D_a, while the image of the lens is retrieved in correspondence of D_b by averaging correlations. In both cases, correlated detection of the two images contains information on the direction of light in the setup, which provides the possibility to recover the image of the object even the focusing conditions (namely, $z_b = z_a$ for S1, and $1/S_1 + 1/S_2 = 1/f$ for S2) are not matched. The common feature of the two setups, represented in Fig. 1, is the fact that light emitted by a chaotic source is split in two paths a and b by a beam splitter (BS), with an object placed in one of the paths, and is recorded at the end of each path by the high-resolution detectors D_a and D_b. More specifically, intensity patterns $i_A(\boldsymbol{\rho}_a)$ and $i_B(\boldsymbol{\rho}_b)$, with $\boldsymbol{\rho}_{a,b}$ the coordinate on each detector plane, are recorded in time to reconstruct the correlation function

$$\Gamma_{AB}(\boldsymbol{\rho}_a, \boldsymbol{\rho}_b) = \langle \Delta i_A(\boldsymbol{\rho}_a)\Delta i_B(\boldsymbol{\rho}_b)\rangle\,, \tag{1}$$

with $\Delta i_{A,B}(\boldsymbol{\rho}_{a,b}) = i_{A,B}(\boldsymbol{\rho}_{a,b}) - \langle i_{A,B}(\boldsymbol{\rho}_{a,b})\rangle$. The expectation value in (1) must be evaluated on the source statistics, but it can be approximated by the time average of the product of intensity fluctuation, provided the source is stationary and ergodic [17]. The lens in S1 focuses the source on the detector D_b, while the lens appearing in S2 focuses the object on D_a. The role of the source is less intuitive: actually, when measuring second-order correlations, a chaotic source

acts as a *focusing element* [14]. In our cases, as will be explained in more detail in the following, the source focuses the object on D_a in S1, and the lens on D_b in S2.
In both setups, the correlation function (1) at fixed $\boldsymbol{\rho}_b$ encodes multiple coherent images of the object. Each point $\boldsymbol{\rho}_b$ on the plane of detector D_b corresponds to a different point of view on the scene, and the images corresponding to different $\boldsymbol{\rho}_b$'s are generally shifted one with respect to the other. If the position of the object in each setup satisfies a specific focusing condition, the relative shift of such images vanishes, and one can integrate over the detector D_b to obtain a total incoherent image, with improved SNR. In all other cases, the images must be realigned before being piled up by integrating over D_b, following

$$\Sigma_{\mathrm{ref}}(\boldsymbol{\rho}_a) = \left\langle \sigma_{(\alpha,\beta)}(\boldsymbol{\rho}_a) \right\rangle, \tag{2}$$

with

$$\sigma_{(\alpha,\beta)}(\boldsymbol{\rho}_a) = \int \mathrm{d}^2\boldsymbol{\rho}_b \Delta i_A(\alpha\boldsymbol{\rho}_a + \beta\boldsymbol{\rho}_b)\Delta i_B(\boldsymbol{\rho}_b). \tag{3}$$

The parameters (α, β), that are necessary to realign the coherent images, depend on the setup. he fluctuations of the observable (3) around their average $\Sigma_{\mathrm{ref}}(\boldsymbol{\rho}_a)$, namely

$$\begin{aligned}\mathcal{F}(\boldsymbol{\rho}_a) &= \left\langle \sigma_{(\alpha,\beta)}(\boldsymbol{\rho}_a)^2 \right\rangle - \left\langle \sigma_{(\alpha,\beta)}(\boldsymbol{\rho}_a) \right\rangle^2 \\ &= \int \mathrm{d}^2\boldsymbol{\rho}_{b1}\mathrm{d}^2\boldsymbol{\rho}_{b2}\Phi(\boldsymbol{\rho}_a, \boldsymbol{\rho}_{b1}, \boldsymbol{\rho}_{b2}),\end{aligned} \tag{4}$$

with Φ a positive function related to the local fluctuations of intensity correlations [compare with the definition of (3), to obtain an estimate of the signal-to-noise ratio related to the refocused images retrieved in S1 and S2. We have achieved interesting properties of the signal-to-noise ratio for the setups S1 and S2, finding that the results obtained for the latter are generally more advantageous than the former. In the focused case, S2 is characterized by the suppression of background noise, that, on the other hand, is a typical feature affecting the ghost image obtained in S1. Moreover, noise in S1 increases with improving resolution on the object entailing a trade-off between resolution and SNR trade-off. In the out-of-focus case, background noise is present in both configurations. However, in S1 it depends on small quantities, namely the ratios between the area of an effective resolution cell and the total area of the object. In S2, instead, we find that the SNR depends also on the ratio between the effective lens area and the one of the object, a quantity that is not necessarily small. Therefore, we expect that a smaller number of frames is needed to achieve the same resolution in S2 compared to S1. The outcomes provide the experimenter with rules to determine the scaling of the SNR with the number of frames, and consequently to fix the number of frames needed for a fast and accurate imaging of the scene. The problem of optimizing the acquisition time is particularly relevant if unconventional sources like X rays [15, 16], characterized by additional difficulties in retrieving intensity correlations, will be employed to

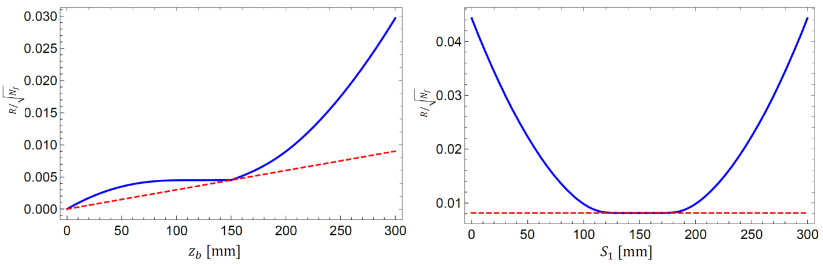

(a) (b)

Figure 2: SNR for the refocused image (2) (solid blue line), and for a ghost image (red dashed line) for SETUP1 (up) and SETUP2 (down) taken at $z_a = z_b$ (for S1) and at $S_2^f = (1/f - 1/S_1)^{-1}$ (for S2) as a function respectively of z_b and S_1.

perform CPI.

Beyond this work, I am working on the proposal to measure the distance of two distant double-slits by analyzing the second-order interference effects of chaotic light. Moreover we would like to include turbulence effects for studying the robustness of the interference pattern.

Referring to figure of the setup, I consider the case in which the two slits are parallel to the horizontal axis, and thus specialize to a quasi-one-dimensional problem. Assuming that the finite size of lenses in both optical paths can be neglected, since the propagation of low horizontal frequencies is only limited by diffraction at the slits. Up to an irrelevant constant, the correlation between intensity fluctuations at the coordinate x_C on the detector D_C and x_T on D_T reads

$$\begin{aligned}\Gamma(x_C, x_T) &= \langle \Delta I_C(x_C) \Delta I_T(x_T) \rangle \\ &= \left| \int \mathrm{d}x_s \, \mathcal{S}(x_s) g_T(x_T, x_s) g_C^*(x_C, x_s) \right|^2 , \end{aligned} \tag{5}$$

where $\mathcal{S}$ is the intensity profile of the source and $g_{C,T}$ are the paraxial transfer functions on each path., which read

$$g_J(x_J, x_S) \propto \exp\left(\frac{\mathrm{i}k}{2} \left(\frac{x_T^2}{f} + \frac{x_s^2}{z_J} \right) \right) \tag{6}$$

The above results are the basic elements to compute the correlation function (5) and its fluctuations.

The expectaion value on the pseudothermal state appearing in Eq. (5) is practically estimated by averaging over the products of intensities $\{I_J^{(i)}\}_{i=1,\ldots,\mathcal{N}}$ measured in correspondence of a set of discrete times $\{t_i\}_{i=1,\ldots,\mathcal{N}}$:

$$\Gamma^{(\mathcal{N})}(x_C, x_T) = \frac{1}{\mathcal{N}} \sum_{i=1}^{\mathcal{N}} \Delta I_C^{(i)}(x_C) \Delta I_T^{(i)}(x_T), \tag{7}$$

with

$$\Delta I_J^{(i)}(x_J) = I_J^{(i)}(x_J) - \frac{1}{\mathcal{N}} \sum_{\ell=1}^{\mathcal{N}} I_J^{(\ell)}(x_J). \tag{8}$$

The correspondence is valid provided intensity fluctuations in the same detection point at different times are uncorrelated with good approximation, namely when $t_{i+1} - t_i > \tau_c$. The asymptotic covariance of the estimation of $\Gamma(x_C, x_T)$ through Eq. (7) is related to the four-point fluctuation correlator as

$$\begin{aligned} \mathcal{C}(x_C, x_T, x'_C, x'_T) &= \mathrm{cov}\{\Gamma^{(\mathcal{N})}(x_C, x_T), \Gamma^{(\mathcal{N})}(x'_C, x'_T)\} \\ &\simeq \frac{1}{\mathcal{N}} \Big(\langle \Delta I_C(x_C) \Delta I_T(x_T) \Delta I_C(x'_C) \Delta I_T(x'_T) \rangle \\ &\quad - \Gamma(x_C, x_T) \Gamma(x'_C, x'_T) \Big), \end{aligned} \tag{9}$$

which comprises the variance $\mathcal{V}(x_C, x_T) = \mathcal{C}(x_C, x_T, x_C, x_T)$ as a special case. I skip the detail for the most general case for $z_T \neq z_C$. Since the number of paramenter are not easy-hand I analyse the behavior of the pattern fixing each parameter time by time. 1) $\bar{X}_T = \bar{X}_C = 0; d_T = d_C; z_T$ finding the firt order of Eq. (5) around z_C;2) $\bar{X}_T = \bar{X}_C = 0; z_T = z_C; d_T$ finding the firt order of Eq. (5) around d_C;3) characterization of the oscillation slope respect to bisector line;4) characterization of the distance between the maximum in the modulation regime; 5) Characterization of the second modulation regime;6) In the semiclassical limit ($\sim$ 100 photons per mode) we can unbalanced the intensity along one of the branch (minimum absorption rate VS SNR); 7) the best settings for the trade-offs; 8) minimum d_T measurable, it turns out the lower bound for the resolution; maximum d_T in order to determine the field of view microscope and by the difference $(d_t - d_c)$ we can analyse the precision of the setup thought as a microscope.

QED in the media

Besides the topics outlined in the preceding part of this report, I am recently investigating from the first principles of quantum electrodynamics QED, a two-level asymmetric quantum system hosted in the bulk of a lossy dispersive media. In particular, I would like to characterize the spontaneous emission rate and the Lamb shift in terms of the asymmetry due to the intrinsic permanent dipole moment. In the free space, the asymmetry do not contribute in the decay rate, but in well-engineered materials the asymmetric nanostructure becomes much more relevant and we predict new contributions which pave the way for new physical phenomena and devices. The asymmetry emerges as a quantum piezoelectric effect of our guest system and all the divergences are overcome by considering the dipole wavefunctions. The general theoretical framework is administer to an hydrogen-like system and to a prominent semiconductor quantum well. Modelling the atom as a dipole of charge Q, with a heavy positive charge in the fixed position $\boldsymbol{R} = 0$ and a moving negative charge of mass m and

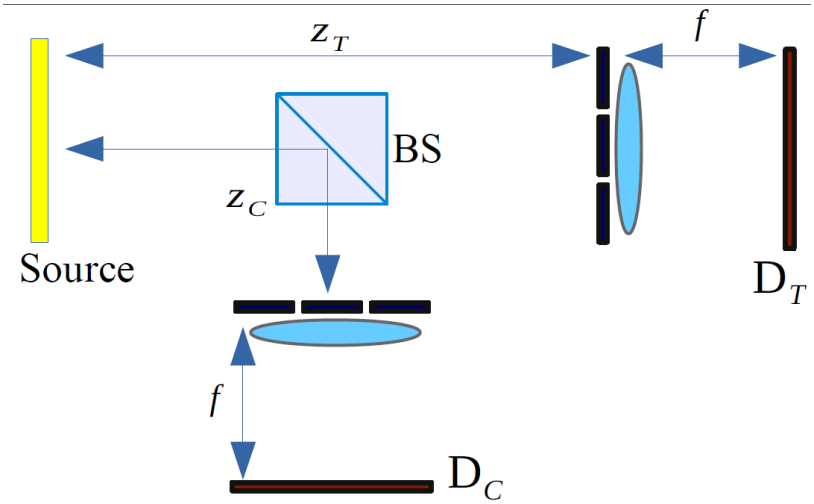

(a)

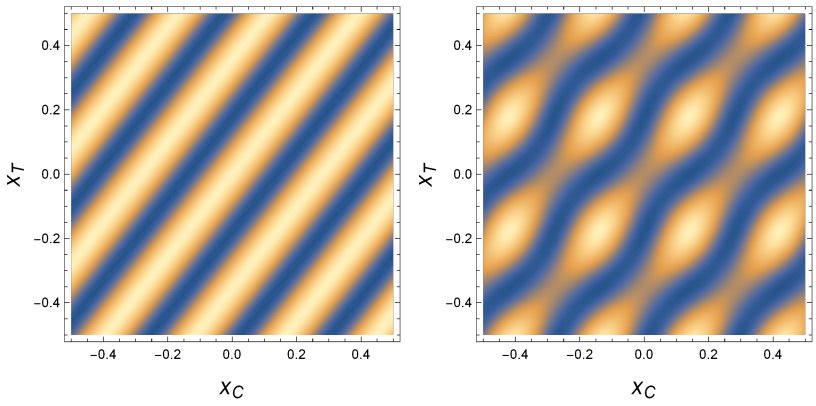

(b) $z_T = z_C$ (c) $z_T = 2.07\, z_C$

Figure 3: Plots of the correlation function $\Gamma(x_C, x_T)$ at different values of the distance z_T of the target slit. The color scale ranges from blue ($\Gamma = 0$) to white (Γ equal to its maximum). The functions are computed with fixed parameters $\lambda = 980\,\text{nm}$, $d_C = 0.70\,\text{mm}$, $d_T = 0.55\,\text{mm}$, $\sigma = 0.55\,\text{mm}$, $z_C = 70\,\text{mm}$, $f = 200\,\text{mm}$, $\bar{X}_C = \bar{X}_T = 0$.

coordinate $-\boldsymbol{\rho}$, one finds the dipole Hamiltonian

$$H_{\rm int}^{\rm dip} = \frac{Q}{\epsilon_0}\boldsymbol{\rho}\cdot\int_0^1 {\rm d}s\,\boldsymbol{\Pi}(-s\boldsymbol{\rho}), \tag{10}$$

representing the correct generalization of the Hamiltonian $\boldsymbol{d}\cdot\boldsymbol{\Pi}$ to a non-point dipole, which regularizes the ultraviolet divergences. Now we can provide an analysis on the dynamics of the Hamiltonian determining the decay rate and the Lamb shift. In my theoretical framework the following quantity determines the total decay rate of the excited state a

$$\begin{aligned}\Gamma_a &= \frac{2\pi}{\hbar}\sum_b\int_0^\infty {\rm d}\omega\delta(\hbar\omega-\hbar\omega_{ab})\int {\rm d}^3\boldsymbol{q}\,\mathcal{T}_{ab}(\boldsymbol{q},\omega)\\ &= \frac{2\pi}{\hbar^2}\sum_{b\neq a}\theta(\omega_{ab})\int {\rm d}^3\boldsymbol{q}\,\mathcal{T}_{ab}(\boldsymbol{q},\omega_{ab}),\end{aligned} \tag{11}$$

where $\omega_{ab} = (E_a - E_b)/\hbar$ [in the second equality, we have considered that $\mathcal{T}_{aa}(\boldsymbol{q},\omega\to 0)\to 0$], and the total energy shift

$$\begin{aligned}\hbar\Delta_a = &\int_0^\infty {\rm d}\omega\frac{1}{\omega}\int {\rm d}^3\boldsymbol{q}\,\bar{\mathcal{T}}_{aa}(\boldsymbol{q},\omega)\\ &+\sum_{b\neq a}{\rm P}\int_0^\infty {\rm d}\omega\frac{1}{\omega-\omega_{ab}}\int {\rm d}^3\boldsymbol{q}\,\mathcal{T}_{ab}(\boldsymbol{q},\omega),\end{aligned} \tag{12}$$

where we have removed a divergent and state-independent part by replacing $\mathcal{T}_{aa}$ with

$$\begin{aligned}\bar{\mathcal{T}}_{aa}(\boldsymbol{q},\omega) &= \mathcal{T}_{aa}(\boldsymbol{q},\omega).\\ &-\frac{Q^2\hbar\epsilon_I(\omega)}{(2\pi)^3\pi\epsilon_0|\boldsymbol{q}|^2|\epsilon(\omega)|^2}\left(1-\frac{1}{\left|1-\frac{|\boldsymbol{q}|^2c^2}{\omega^2\epsilon(\omega)}\right|^2}\right).\end{aligned} \tag{13}$$

The $\mathcal{T}$ is the sum of the element matrix $\mathcal{M}$ as follows

$$\mathcal{T}_{ab}(\boldsymbol{q},\omega) = \sum_{j=1}^3\left|\mathcal{M}_j^{ab}(\boldsymbol{q},\omega)\right|^2, \tag{14}$$

with

$$\begin{aligned}\mathcal{M}_j^{ab}(\boldsymbol{q},\omega) &= \langle a|H_{\rm int}^{\rm dip}|b;(\boldsymbol{q},\omega)_j\rangle = \langle a|H_{\rm int}^{\rm dip}f_j^\dagger(\boldsymbol{q},\omega)|b\rangle\\ &= C_{\mathcal{M}}\tilde{G}_{jk}(\boldsymbol{q},\omega)\langle a|r_k\int_0^1 ds{\rm e}^{-{\rm i}s\boldsymbol{q}\cdot\boldsymbol{\rho}}|b\rangle,\end{aligned} \tag{15}$$

and $C_{\mathcal{M}} = -{\rm i}Q\frac{\omega^2}{c^2}\sqrt{\frac{\hbar\epsilon_I(\omega)}{(2\pi)^3\pi\epsilon_0}}$. The quantity $\tilde{G}_{jk}$ is the well-know *tensor green function* which I have already studied during my first year [5]

Quantum correlations

During my period aborad I have worked on the problem of quantum entanglement, which is the essence of many fascinating quantum-mechanical effects. It is a very fragile phenomenon. It is usually very hard to create, maintain, and manipulate entangled states under laboratory conditions. In fact, any system is usually subjected to the effects of external noise and interactions with the environment. These effects turn pure-state entanglement into mixed-state, or noisy, entanglement. The separability problem, that is, the characterization of mixed entangled states, is highly nontrivial, and has not been accomplished so far. Even an apparently innocent question -*Is a given state entangled and does it contain quantum correlations, or is it separable, and does not contain any quantum correlations?*?will, in general, be very hard (if not impossible!) to answer. In this scenario I provide a new family of separability criteria both for bipartite and multipartite quantum systems with arbitrary (but finite) dimensions of the corresponding Hilbert spaces. This criterion unifies several known separability criteria: the powerful realignment (or CCNR) criterion which is able to detect many bound entangled state or the criterion derived by de Vicente. Surprisingly, the recently proposed criterion based on symmetric informationaly complete measurements SIC POVMs (so called ESIC criterion) turns out to be a special example of our criterion. Moreover, our result shows that this criterion is universal, that is, it does not require the existence of SIC POMV at all!

Its characteristic feature is that unlike other criteria like e.g. Covariance Matric Criterion (CMC) or Local Uncertainty Relations (LURs), extensions of realignment criterion, is linear in the state of the system. This property allows to derive appropriate family of entanglement witnesses and new classes of positive maps suitable for entanglement detection.

The generalization to multipartite scenario is also provided. This is based on the generalization of the trace norm from matrices to arbitrary N-tensors (where N is a number of parties). We show that our proposal is stronger that the one already discussed based on the mathematical theory of unfoldings. Moreover, it is conceptually much simpler and physically more intuitive. In particular it provides generalization of CCNR to arbitrary number of parties.

The last point is the detection power: is it stronger than other criteria? It is well known that CCNR criterion does not detect all entangled qubit-qubit state. An example of such state was provided by Rudolph. Now, this state is detected by our criterion. In the end I analyzed well known examples of PPT entangled states based on the construction of Unextendible Product Bases showing that our criterion is stronger than CCNR and ESIC. Clearly, being linear criterion in general it is difficult to be compared with nonlinear ones like e.g. CMC or LURs. However, we provide an example of qutrit-qutrit PPT state which is detected neither by CCNR, nor by CMC supplemented by local filtering but is perfectly detected by my criterion brefly explain in the following just for the bipartite case for semplicity.
Consider a bipartite system living in $\mathcal{H}_A \otimes \mathcal{H}_B$ with dimensions d_A and d_B, respectively. Let G_α^A and G_β^B denote arbitrary orthonormal basis in $\mathcal{B}(\mathcal{H}_A)$ and

$\mathcal{B}(\mathcal{H}_B)$, that is, the $\mathrm{Tr}(G_\mu^{A\dagger} G_\nu^A) = \delta_{\mu\nu}$, and the same for G_β^B. Now, given a bipartite state ρ one defines the following correlation matrix

$$C_{\alpha\beta} = G_\alpha^A \otimes G_\beta^B \ = \mathrm{Tr}(\rho G_\alpha^A \otimes G_\beta^B). \tag{16}$$

If ρ is separable, then the CCNR criterion gives the following bound for the trace norm of C:

$$\|C\|_{\mathrm{tr}} \equiv \mathrm{Tr}\sqrt{CC^\dagger} \leq 1. \tag{17}$$

The norm $\|C\|_{\mathrm{tr}}$ does not depend upon the particular orthonormal basis G_α^A and G_β^B. Let us take a particular basis consisting of Hermitian operators such that $G_0^A = \mathbb{1}_A/\sqrt{d_A}$ and $G_0^B = \mathbb{1}_B/\sqrt{d_B}$ (we call it canonical basis). It is clear that G_α^A and G_β^B are traceless for $\alpha, \beta > 0$. The canonical basis gives rise the following generalized Bloch representation

$$\begin{aligned} \rho \ &= \ \frac{1}{\sqrt{d_A d_B}} G_0^A \otimes G_0^B + \sum_{i>0} r_i^A G_i^A \otimes \mathbb{1}_B + \sum_{j>0} r_j^B \mathbb{1}_A \otimes G_j^B \\ &+ \ \sum_{i,j>0} t_{ij}\, G_i^A \otimes G_j^B = \sum_{\alpha=0}^{d_A^2-1} \sum_{\beta=0}^{d_B^2-1} C_{\alpha\beta}^{\mathrm{can}} G_\alpha^A \otimes G_\beta^B, \end{aligned} \tag{18}$$

where r_i^A and r_j^B are generalized Bloch vectors corresponding to reduces states ρ_A and ρ_B, respectively, and t_{ij} is usually called a correlation tensor. We denote $C_{\alpha\beta}$ defined by the canonical basis by $C_{\alpha\beta}^{\mathrm{can}}$. Clearly $\|C^{\mathrm{can}}\|_{\mathrm{tr}} = \|C\|_{\mathrm{tr}}$. Let us introduce two square diagonal matrices:

$$D_x^A = \mathrm{diag}\{x, 1, \ldots, 1\}, \quad D_y^B = \mathrm{diag}\{y, 1, \ldots, 1\},$$

where D_x^A is $d_A^2 \times d_A^2$ and D_y^B is $d_B^2 \times d_B^2$. Now comes the main result

Theorem 1 *If ρ is separable, then*

$$\|D_x^A C^{\mathrm{can}} D_y^B\|_{\mathrm{tr}} \leq \mathcal{N}_A(x)\mathcal{N}_B(y), \tag{19}$$

where

$$\mathcal{N}_A(x) = \sqrt{\frac{d_A - 1 + x^2}{d_A}} \quad \mathcal{N}_B(y) = \sqrt{\frac{d_B - 1 + y^2}{d_B}}, \tag{20}$$

for arbitrary $x, y \geq 0$.

In the future I would like spent my efforts towards the *only if* direction and investigate correlations beyond quantum mechanics, in jargon *out of the polytope* in order to answer at the following question:

Is quantum mechanics the last universal theory of the nature?

Training activities

I did all my exams and also attended the following schools and conferences:

- *51st Symposium on Mathematical Physics*, Toruń (Poland), 16–18 June 2019, with presentation of the talk "The Friedrichs-Lee model and its singular coupling limit";
- *Summer School: Topics in Quantum Probability*, Genoa, 1–3 July 2019;
- *Introductory Course on UltracoldQuantum Gases*, Innsbruck (Austria), 8–10 July 2019;
- *Italian Quantum Information Science conference*, Milan, 9–12 September 2019, with presentation of the poster "Bound states in the continuum for an array of quantum emitters".
- *YQIS 2019: 5th International Conference for Young Quantum Information Scientists*, University of Gdansk, Sopot, Poland, September 25-27, 2019.

References

[1] C. Cohen-Tannoudji, J. Dupont-Roc, and G. Grynberg, *Atom-Photon Interactions: Basic Processes and Applications* (Wiley, Chichester, 1998)

[2] M. Lewenstein, B. Kraus, J. I. Cirac, and P. Horodecki, "Optimization of entanglement witnesses", PHYSICAL REVIEW A, VOLUME 62, 0523101 Institute for Theoretical Physics, University of Hannover, D-30167 Hannover, Germany

[3] R.F. Werner, Phys. Rev. A **40**, 4277 (1989).

[4] C. Wu, J. Ko, and C. C. Davis, "Imaging through strong turbulence with a light field approach," Opt. Express **24**, 11975 (2016).

[5] A. Tip, L. Knöll, S. Scheel, D.G. Welsch, Phys. Rev. A 63(4), 043806 2001.

[6] M. D'Angelo, F. V. Pepe, A. Garuccio, and G. Scarcelli, "Correlation Plenoptic Imaging," Phys. Rev. Lett. **116**, 223602 (2016).

[7] F. V. Pepe, G. Scarcelli, A. Garuccio, and M. D'Angelo, "Plenoptic imaging with second-order correlations of light," Quantum Meas. Quantum Metrol. **3**, 20 (2016).

[8] F. V. Pepe, F. Di Lena, A. Garuccio, G. Scarcelli, and M. D'Angelo, "Correlation plenoptic imaging with entangled photons," Technologies–Open Access Multidisciplinary Engineering Journal **4**, 17 (2016).

[9] F. V. Pepe, F. Di Lena, A. Mazzilli, E. Edrei, A. Garuccio, G. Scarcelli, and M. D'Angelo, "Diffraction-Limited Plenoptic Imaging with Correlated Light," Phys. Rev. Lett. **119**, 243602 (2017).